# Noise-induced coherent oscillations in randomly connected neural networks

J. Pham,[1] K. Pakdaman,[1,2] and J.-F. Vibert[1]
[1]*B3E, INSERM U 444, ISARS, UPMC Faculté de Médecine Saint-Antoine, 27, rue Chaligny, 75571 Paris Cedex 12, France*
[2]*Department of Biophysical Engineering, Faculty of Engineering, Osaka University, Toyonaka, Osaka 560, Japan*
(Received 11 February 1998)

We study the dynamics of randomly connected excitatory networks of excitable spike-response neuron models. Large networks can exhibit a nonmonotonic collective response to a stimulation when the coupling strength between neurons lies within an appropriate range. With such a coupling, noise imposed upon neurons induces synchronization of the units and oscillations of the network activity, consisting of a succession of bursts. Furthermore, the regularity of this rhythmic activity goes through a maximum as the noise amplitude is increased. This nonmonotonic dependence on the noise amplitude relies on the fact that noise acts in two antagonistic ways. Noise of low amplitude shortens the interval between two successive bursts, leading to an increase of the dynamics regularity, whereas noise of strong amplitude deteriorates the regularity of the dynamics during a burst. In order to study the influence of the noise amplitude and the coupling on the generation of collective oscillations quantitatively, we consider a simpler network model of excitable units. We derive a discrete map, including the noise amplitude and the coupling strength as parameters, which describes the network dynamics in the limit of a large number of neurons. This map reproduces all characteristic features of the activity dynamics obtained with simulated networks. From the analysis of the bifurcation structure of this map, we obtain parameter regions where noise-induced oscillations occur. Using this map we also study the effect of the network connectivity on the generation of oscillations. We show that such noise-induced coherent oscillations in fully connected networks are related to special initial conditions, and are sensitive to perturbations, whereas they can be the only asymptotically stable regime in sparsely connected networks. [S1063-651X(98)06909-8]

PACS number(s): 87.10.+e, 07.05.Mh

## I. INTRODUCTION

The presence of noise can influence information processing by nerve cells (for a review, see Ref. [1]) in several ways. For instance, noise can linearize a neuron's input-output transfer function in response to suprathreshold sine-like periodic inputs [2]. Noise can also smooth the neuron's response to steplike inputs [3]. The mechanisms of these effects have been analyzed theoretically [4].

Noise of an appropriate level may also help neurons to detect subthreshold periodic [5] or aperiodic signals [6]. Extensive theoretical studies of this noise effect have been carried out [7]. These have shown that stochastic resonance (SR) may be one possible mechanism by which noise modifies signal processing in neurons. SR means that an optimal level of noise maximizes the regularity of the neuron spike train, or maximizes the fidelity of its response to a subthreshold input. For instance, one manifestation of SR occurs when there is matching between the time scale of the noise-induced firings and the input signal period or the period of some autonomous subthreshold oscillations [8]. Thus one striking effect of SR is that, for an appropriate range of noise amplitude, the neuron generates a close to periodic spike train. Such a behavior is related to the periodic nature of the input.

Meanwhile, noise-induced coherent dynamics have also been reported in the absence of periodic modulation. Sigeti and Horsthemke [9] showed that an excitable ring device, when placed close to a saddle-node bifurcation, displays oscillations with a dominant frequency. Another numerical work was later carried out by Rappel and Strogatz [10], who considered a system with two simultaneous saddle-node bifurcations. They observed that, close to such a bifurcation, noise accelerates the slow parts of the trajectories, so that the oscillation frequency increases with the noise amplitude. This work followed the numerical investigations of the same system by Gang *et al.* [11], who moreover reported that the coherence of these oscillations was maximized at an intermediate noise amplitude. Therefore, this work showed the existence of SR in an autonomous system, i.e., in a system without external forcing.

As pointed out by Rappel and Strogatz, a key feature in these results was the differential response of slow and fast dynamics to external fluctuations. The importance of this factor in noise-induced coherence was further confirmed by Pikovsky and Kurths [12]. These authors analyzed the response of the FitzHugh neuron model in the excitable regime under the sole influence of white Gaussian noise. They reported that various measures of the regularity of this system's dynamics were maximized at an intermediate noise amplitude. Pikovsky and Kurths showed that, in response to noise of low amplitude, the discharges were highly irregular, due mainly to the large variability in the first passage time between the resting state and the firing threshold. Increasing the noise level regularized the discharges, because it reduced this variability without much affecting the time required for the system to come back to its resting state once an action potential was generated. Higher noise levels, however, distorted this recovery process, and led to an increased variability. In the present study, we show that a similar mechanism can lead to noise-induced coherent activity in networks of neuron models. Regular activities in the presence of noise

 

have already been reported in periodically driven networks of coupled oscillators or excitable units [13].

Noise alone, without periodic input, can also induce synchronized oscillations. This phenomenon was analyzed in networks of globally coupled active rotators [14]. Isolated active rotators switch from excitable to oscillating regimes through a saddle-node bifurcation, and their response to noise is, thus, similar to what has been reported in [9,11,10]. When each excitable unit is close to the saddle-node bifurcation, coherent oscillations appear at intermediate noise levels. Recently, Kurrer and Schulten proposed a new approximation to reexamine this phenomenon, and found similar transitions between coherent and incoherent states at intermediate noise levels [15]. Coupled active rotators interact ''diffusely'' in the sense that the influence of one unit upon another is a smooth function of their phase difference. Yet, even when network units interact by pulses, noise alone can lead to synchronous regular discharges in coupled excitable systems. Rappel and Karma [16] observed this phenomenon in numerical simulations of globally pulse-coupled integrate-and-fire neurons. They showed that the periodicity of the overall network activity is a humped shaped function of the noise amplitude. They also indicated that this phenomenon is more pronounced when the number $N$ of network units is large.

We present a form of noise-induced partial synchronization and coherent collective oscillations in excitatory networks of spike-response neural models [17–19]. In a previous study, we have shown that, with this type of model, the whole network can behave like an excitable system [20]. In this paper, we analyze the influence of noise on the dynamics of such networks. We show that noise can induce collective oscillations, provided the coupling strength of the network units lies within an appropriate range. In this range of coupling, there exists an optimal value of the noise amplitude maximizing the coherence of the oscillations. We also consider a simpler network model whose dynamics can be described by a discrete map. From the bifurcation diagram of this map, we determine the ranges of the coupling and the noise amplitude where coherent oscillations are possible. Theoretical results are in agreement with simulations. Finally, we show that the conditions under which oscillations can be obtained depend on the connectivity of the network, and are quite different with fully or sparsely connected networks.

This paper is organized as follows. The network model and simulation results are described in Sec. II. In Sec. III, we introduce a simplified network model and derive a discrete map that gives its dynamics. Then we analyze the bifurcation structure of this map. In Sec. IV, we examine the effect of connectivity. The paper is concluded in Sec. V.

## II. COHERENT OSCILLATIONS

### A. Network model

The network model used through this study consists of a randomly connected population of $N$ excitable units. When building the network, connections are randomly chosen: neuron $j$ connects to neuron $i$ $(i \neq j)$ with probability $K/(N-1)$, so that each connection $c_{ij}$ is the realization of a Bernoulli random variable of parameter $K/(N-1)$ and $c_{ii}=0$. $K$ will be referred to as the connectivity parameter. It corresponds to the mean number of connections emitted or received by a neuron. Each neuron $i$ $(1 \leqslant i \leqslant N)$ is described by its membrane potential $V_i$. For the sake of convenience $V_i$ is represented in dimensionless units, and the resting value of the potential is set to zero. The neuron sums its inputs over time, since its last discharge time $T_i$. Once $V_i$ overtakes a threshold value $\theta$, the neuron fires, sends outputs to other units, and immediately resets its potential. The neuron model is similar to the spike-response neuron model [17–19] with absolute and relative refractory periods. At time $t$, $V_i(t)$ is given by

$$V_i(t) = -\infty \quad \text{if} \quad 0 \leqslant t - T_i \leqslant t_{\text{ref}}, \tag{2.1}$$

$$V_i(t) = U(t-T_i) + \frac{J}{K} \sum_{j=1}^{N} c_{ij} \int_{T_i}^{t} I_i(u)\,du$$

otherwise,

$$I_i(u) = \sum_{t_j^f > T_i - d_{ij}} \delta(u - d_{ij} - t_j^f)\, v(t-u), \tag{2.2}$$

$$U(t) = U_m \exp(-t/t_m), \tag{2.3}$$

where $t_{\text{ref}}$ is the duration of the absolute refractory period, $J$ is the coupling constant, $t_j^f$ are the firing times of neuron $j$, $U_m$ is the after-spike hyperpolarization, and $t_m$ is the potential recovery time constant which determines the duration of the relative refractory period. $U(t-T_i)$ will be referred to as the refractory state of neuron $i$ at time $t$. When neuron $j$ fires, neuron $i$ receives, after a time delay $d_{ij}$, an excitatory input given by

$$v(t) = 0 \quad \text{if} \quad t < 0,$$

$$v(t) = (t/t_r)\exp(-(t-t_r)/t_r) \quad \text{if} \quad 0 \leqslant t \leqslant t_r,$$

$$v(t) = ((t + t_f - t_r)/t_f)\exp(-(t-t_r)/t_f) \quad \text{if} \quad t > t_r. \tag{2.4}$$

The shapes of two different types of such excitatory-postsynaptic potentials (EPSP's) are presented in Fig. 1. Noise is introduced by giving to a neuron with potential $V_i$ at time $t$ the following probability of firing between $t$ and $t + \delta t$:

$$p = \delta t \rho(\theta - V_i(t)), \tag{2.5}$$

where $\rho$ is a sigmoidal function whose maximal slope decreases with the noise amplitude $\sigma^2$. Such a definition of stochastic firing gives realistic spiking statistics to the neuron model [17].

Through this study, we use the following set of parameters: $\theta = 2.1$, $t_{\text{ref}} = 1$ ms, $K = 15$, $U_m = -8$, $t_m = 25$ ms, and $t_r = 1$ ms, $t_f = 2$ ms. The membrane potential is expressed in the number of EPSP amplitudes. Thus a firing threshold of 2.1 means that a neuron with potential close to the resting value must receive more than two EPSP's within

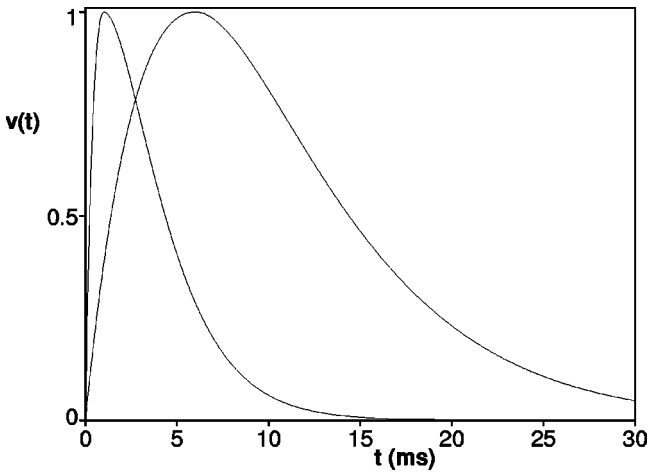


FIG. 1. Excitatory-post-synaptic potential (EPSP) $v(t)$ [Eq. (2.4)] as a function of time $t$ after the firing of a presynaptic neuron. Two different types of EPSP's are presented: short lasting ($t_r = 1$ ms and $t_f = 2$ ms) and long lasting ($t_r = 6$ ms and $t_f = 5$ ms). The potential is normalized by the amplitude of the EPSP, so that $v(t)$ is dimensionless and is between 0 and 1.

a short time interval to discharge. The delays $d_{ij}$ are distributed according to a truncated Gaussian law, over $[1;10]$, of mean $d = 5$ ms and variance 1 ms$^2$. $\rho$ is the Gaussian repartition function with mean zero and variance $\sigma^2$. Network simulations were run with a time step $\Delta t = 0.2$ ms and with $N = 1000$ neurons. Controls run with smaller time steps and larger network sizes led to the same results. In order to follow how spiking evolves during time within the network, we define the activity level $S(t)$ as the total number of spikes in the network, normalized by the number $N$ of units, during the time interval $[t - t_w; t]$ where $t_w = 1$ ms.

### B. Effect of the coupling strength

First we examine the effect of the coupling strength on the network behavior. Figure 2 presents the dynamics of $S$ and the corresponding normalized autocorrelation functions for four values of the coupling constant $J$, with $\sigma^2 = 1$. The normalized autocorrelation at a time lag $l$ ms is defined by

$$C(l) = \frac{\langle \tilde{S}(t)\tilde{S}(t+l)\rangle}{\langle (\tilde{S})^2\rangle}, \quad \tilde{S} = S - \langle S\rangle. \tag{2.6}$$

With a weak coupling ($J = 1$), the activity level $S$ is low and shows only small random fluctuations around its mean, as indicated by the autocorrelation. $S(t)$ is close to the superposition of the independent firing processes of isolated neurons driven by noise. As the coupling increases, spiking of the neurons become less independent, and quite regular oscillations of the activity level appear ($J = 6$). The amplitude of these oscillations increases smoothly with the coupling strength, and the time course of $S$ tends to a succession of bursts of activity ($J = 12$). These oscillations of $S$ indicate a partial synchronization: a non-negligible fraction of the neurons tend to fire simultaneously, or at least within a short time window.

At the beginning of a burst, for most of the neurons, the refractory state $U$ is close to zero [see Fig. 3(a)], and noise brings about the spiking of a few of them. Following these spikes, EPSP's are generated on efferent neurons after about one mean transmission delay $d$. These EPSP's raise the firing probability and lead to more discharges. The activity is in this way amplified, and partial synchronization of the spike trains of the neurons occurs, even though the transmission delays do not all have the same values. The progressive increase of the activity leads to a decrease of the average refractory state of the neurons. This, in turn, prevents a further increase of the activity, which eventually decreases and dies out. At the end of a burst, a large fraction of the neurons have discharged at least once. These neurons progressively regain their excitability as their potential rises, and a new burst can be ignited by noise. Thus the burst is the result of two antagonistic phenomena occurring simultaneously: the amplification of an initial noise-induced firing thanks to the excitatory connections, and the increasing refractoriness of the neurons as $S$ rises.

The interval between two successive bursts is mainly related to the duration of the relative refractory period. The duration of a burst depends on the coupling strength $J$ and on the mean transmission delay $d$, which both determine the speed of the spiking amplification. The duration of a burst is also related to the duration of an EPSP. Long lasting EPSP's lead to long bursts [see Fig. 3(b)]. Actually, bursts can be obtained over wide ranges of the network model parameters. We also want to stress that this rhythmic activity is not due to an intrinsic tendency of the network to oscillate. If noise is suppressed during the simulation, oscillations disappear. Indeed, when the coupling is not strong enough, the network is not able to maintain a sustained firing through reexcitatory loops between the neurons without noise. The network can only transiently amplify the neurons' firing: during a burst, after a temporary increase, the firing is brought down by the refractoriness of the neurons. If noise is present, when neurons regain their excitability, a new burst can be induced. If noise is not present, the firing will die out. Moreover, without noise, whatever the initial condition is, the spiking rapidly dies out after a few iterations and no oscillations are obtained.

When the coupling is strong ($J = 16$, Fig. 2), once ignited by noise, the activity rapidly grows up and remains at a high level. A large fraction of the neurons discharge with a high frequency. In this case, even if the noise is suppressed during the simulation, the activity is maintained at a high level.

Thus there are three different types of regimes according to the network coupling strength: low constant activity level for weak values of $J$, high constant activity level for strong values of $J$, and oscillations for intermediate coupling. When the coupling strength is in high intermediate values ($J = 14.3$, for instance), depending on the initial condition, a network can either present oscillations or a high constant activity level. For such values of the coupling the high constant activity level state is very stable once settled. Meanwhile, obtaining this steady state requires that a large fraction of the neurons fire simultaneously at a given time. With high intermediate values of $J$ such a synchronization may be achieved only very rarely due to noise, so that oscillation can last for a very long time. When the coupling $J$ is in-

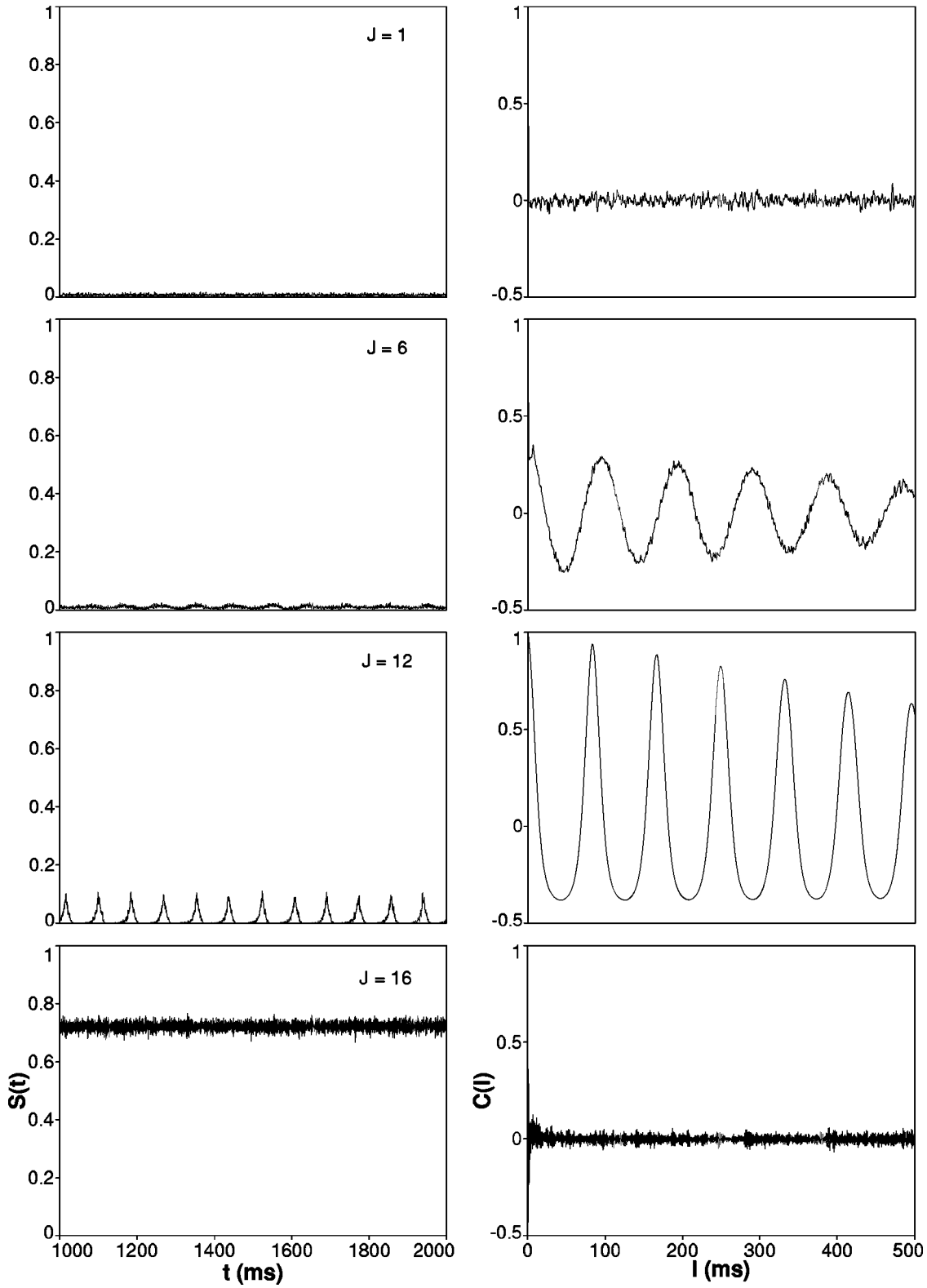


FIG. 2. Time course of the activity level $S(t)$ (dimensionless) (left) and corresponding normalized autocorrelation functions (dimensionless) (right) in simulated networks with $\sigma^2=1$, and for different values of the coupling $J$. $S(t)$ is the total number of discharges occurring between $t-1$ ms and $t$ normalized by the number $N$ of neurons. Network simulations [Eqs. (2.1)–(2.4)] were performed with a time step $\Delta t=0.2$ ms and $N=1000$ units. Autocorrelation functions were computed using 20 000 values.

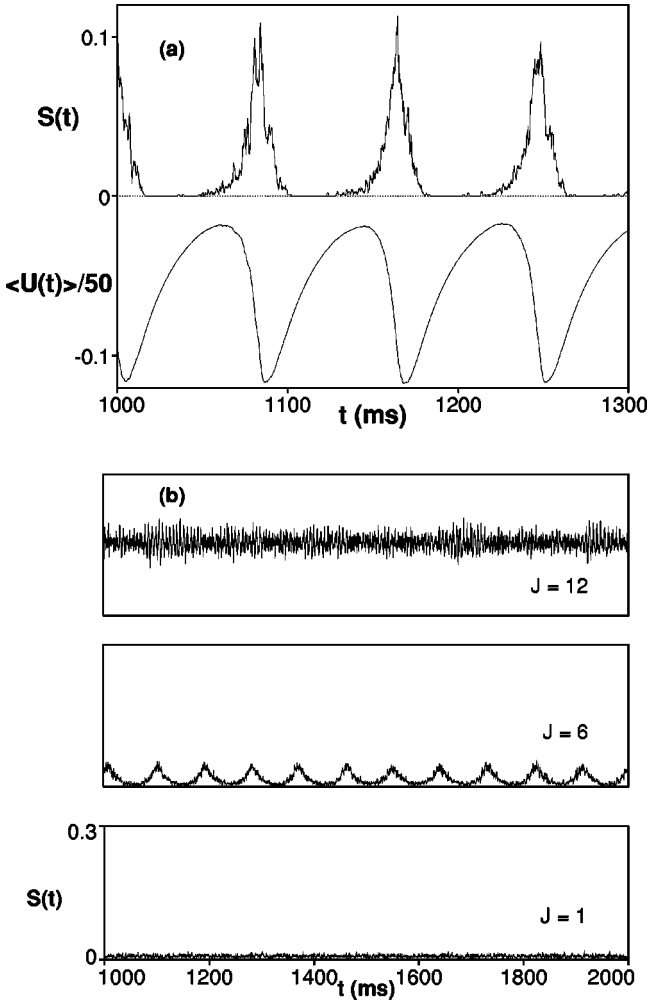


FIG. 3. (a) Activity level $S(t)$ (dimensionless) of a simulated network [Eqs. (2.1)–(2.4)] and mean refractory state $\langle U(t)/50 \rangle$ (dimensionless) of this network as a function of time $t$, with $J=12$, $\sigma^2=1$, $N=1000$, and a time step $\Delta t=0.2$ ms. (b) Time course of the activity level $S(t)$ of simulated networks, for different coupling constants $J$, in the case of long lasting EPSP's: $t_r=6$ ms and $t_f=5$ ms (see Fig. 1).

creased, synchronization is facilitated, and noise brings the system more easily and quickly to the high constant activity level state.

### C. Effect of the noise amplitude

We now examine the effect of the noise amplitude on the generation of oscillations. Figure 4 presents the coherence $H$ of $S$ as a function of $\sigma^2$ for three different values of the coupling. $H$ is defined as the highest peak value obtained in the power spectrum of $S(t)$. This value is normalized by the sum of the spectrum components $\langle S^2 \rangle$. With a strong coupling ($J=16$), noise has little effect on the coherence. With intermediate values of $J$ ($J=7$ or 12), $H$ is maximized as $\sigma^2$ goes through an optimal value.

Figure 5 presents the dynamics of $S$ for four different noise amplitudes with $J=12$. With a very low noise amplitude ($\sigma^2=0.3$), bursts are not present. When $\sigma^2$ is varied from 0.3 to 0.4, bursts abruptly appear. With $\sigma^2=0.4$, the interval between two successive bursts is quite variable. As

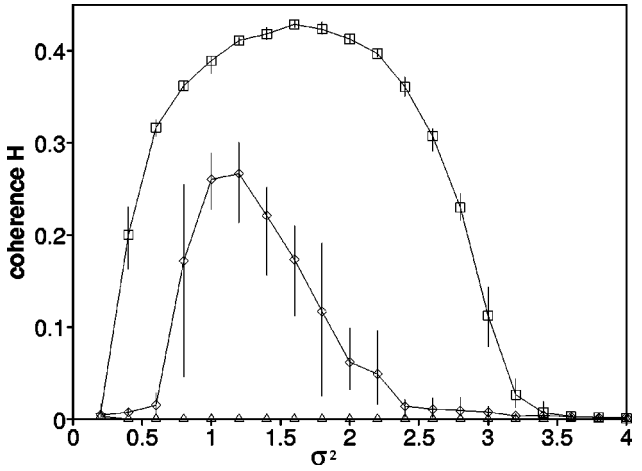


FIG. 4. Coherence $H$ (dimensionless) of the activity level of simulated networks as a function of the noise amplitude $\sigma^2$, for different coupling constants: △, $J=16$; ◇, $J=7$; □, $J=12$. Each point is the average coherence obtained over ten networks. Vertical lines indicate the lowest and highest values of $H$ obtained with the ten networks. $H$ is defined as the highest peak value in the power spectrum, computed with the activity level $S(t)$, normalized by the sum of the spectrum components. Power spectra were computed using 16 384 values of $S$ sampled at 0.2 ms.

the noise amplitude becomes larger, the interburst interval becomes shorter and less variable. With medium noise amplitudes ($\sigma^2=1.6$), as soon as a burst is finished a new one starts, and the activity level dynamics is very regular. With large noise amplitudes ($\sigma^2=3.5$) the amplitude of the oscillations is small, and the activity dynamics is less regular.

The nonmonotonic dependence of the oscillations' coherence on the noise amplitude, can be interpreted in the following way. The whole network is an excitable system, in the sense that it has two different ways of responding to a stimulation consisting of the spiking of a few neurons [20]. If the stimulation is too weak, the firing is not amplified. If the stimulation is large enough, it leads to a burst. Noise of very small amplitude cannot trigger such a transient amplification of the activity level. When $\sigma^2$ is larger bursts become possible, thanks to the noise which acts at two levels. First, at the beginning of a burst, the initial noise induced firing is larger than a threshold level (enough neurons spiking within a short time interval), which leads to the rapid amplification of the firing. Second, noise decreases this threshold level by increasing the firing probability of a neuron receiving a subthreshold input.

With low noise amplitudes, bursts are ignited by the noise-induced firing of neurons receiving no inputs. Consequently, the interburst interval is related to the interspike interval of an isolated neuron driven by noise, which becomes shorter and less variable as $\sigma^2$ increases. Thus, when $\sigma^2$ increases, the interburst interval becomes shorter and more regular. Conversely, noise of low amplitude does not significantly alter the time course of $S$ during a burst. Therefore, when $\sigma^2$ is varied from 0.4 to 1.6, the activity coherence is raised.

With large noise amplitudes, the firing probability of a refractory neuron receiving a subthreshold input is nonnegligible. Consequently, the spiking of a neuron during a burst becomes less related to its inputs. Hence, with large

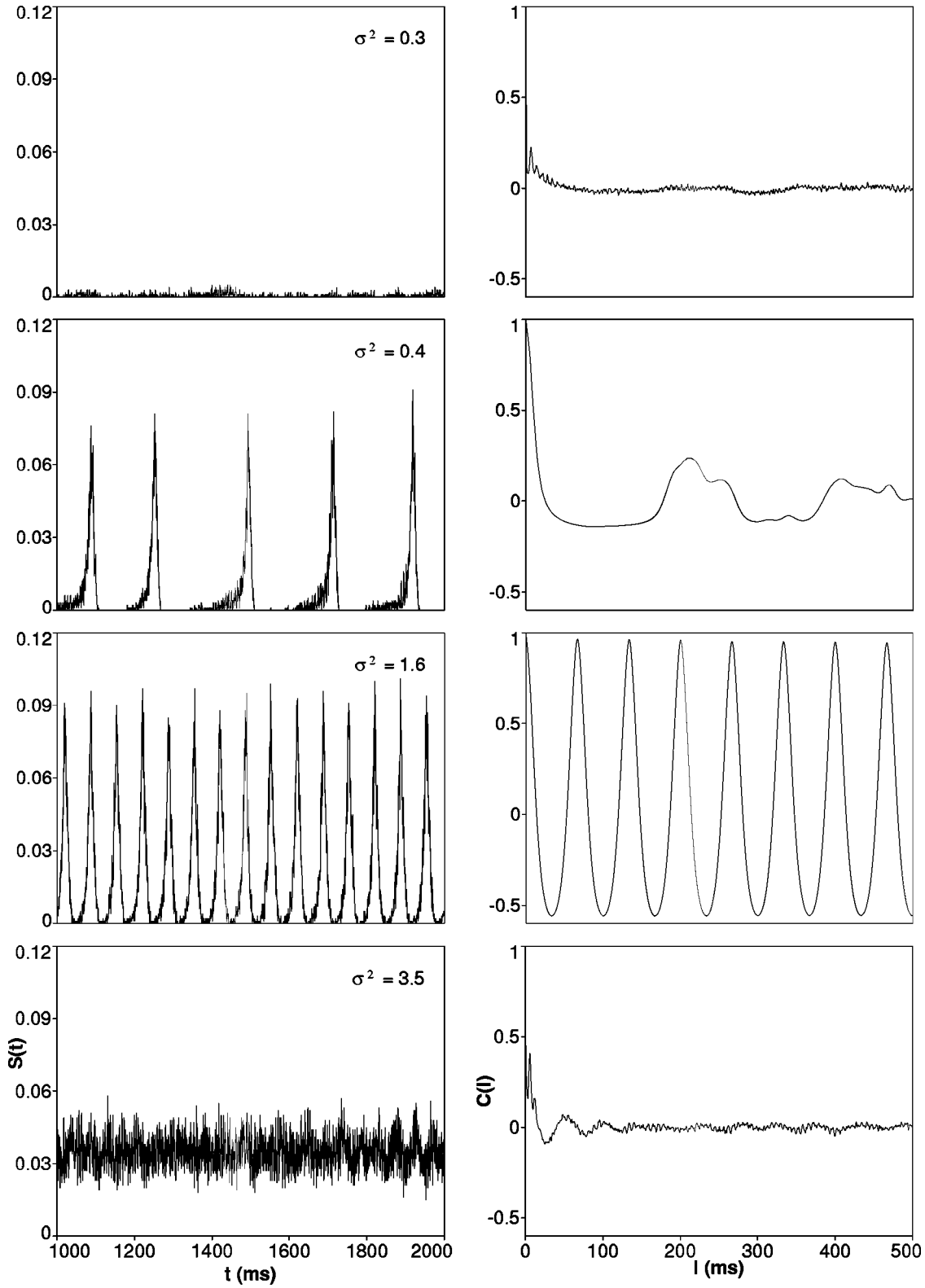


FIG. 5. Time course of the activity level $S(t)$ (dimensionless) (left) and corresponding normalized autocorrelation functions (dimensionless) (right) in simulated networks with $J=12$, and for different values of the noise amplitude $\sigma^2$. Network simulations [Eqs. (2.1)–(2.4)] were performed with a time step $\Delta t=0.2$ ms and $N=1000$ units. Autocorrelation functions were computed using 20 000 values of $S$.

noise amplitudes, the activity level $S(t)$ becomes less correlated to $S(t-d)$, and the coherence decreases. Therefore, noise of small amplitude raises the coherence by shortening the interburst interval, and noise of large amplitude lowers it by spoiling the dynamics during the bursts.

Moreover, with large values of $\sigma^2$, bursts tend to disappear. This is shown in Fig. 6, where the average amplitude and the period of the oscillations are presented as a function of $\sigma^2$. Oscillations appear brutally, with a sharp rise of their amplitude, as $\sigma^2$ increases. Once the bursts have appeared,

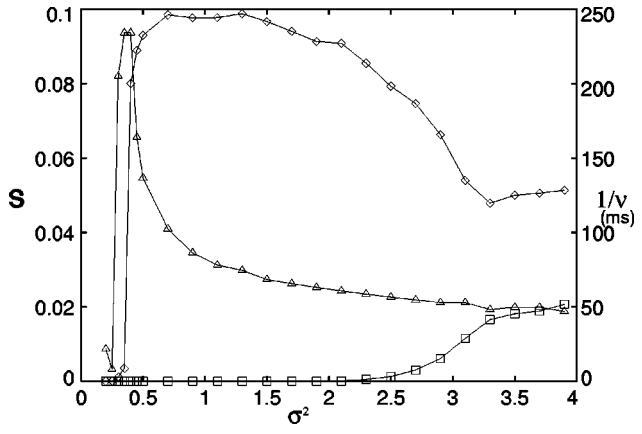


FIG. 6. Characteristics of the oscillations of the activity level $S$ in a simulated network ($N=1000$, $J=12$, and $\Delta t=0.2$ ms) as a function of the noise amplitude $\sigma^2$. The period ($\triangle$) of the oscillations is defined as the inverse of the dominant frequency $\nu$ obtained with the power spectrum of $S(t)$. The average minimal ($\square$) and maximal ($\diamond$) values of $S$ during oscillations were obtained by averaging all the values $S(t)$ (dimensionless) which are local minima and maxima over a time window of width $1/\nu$ c entered in $t$.

the period of the oscillations monotonously decreases with $\sigma^2$. The amplitude stays large until $\sigma^2$ is close to 1.5, and then it decreases. In Sec. III by considering a simpler model, we derive a map whose dynamics have the same dependence on the noise amplitude. Such a map allows us to determine quantitatively which values of the noise amplitude and of the coupling strength lead to noise-induced oscillations.

## III. REDUCTION TO A MAP

We now consider a simpler network model having all the essential properties of the previous model. That is, the network is made of $N$ pulse-coupled excitatory excitable units having a relative refractory period. To simplify the model we consider that all the connections have the same transmission delay, greater than the duration of the absolute refractory period. We also set a finite duration $n$ of the relative refractory period. The neurons update their potential in discrete time:

$$V_i^t = U(t-T_i) + \frac{J}{K}\sum_{j=1}^{N} c_{ij} a_j^{t-1} + B_i^t, \tag{3.1}$$

$$U(t) = U_m \exp(-t/t_m) \quad \text{if} \quad t<n, \tag{3.2}$$

$$U(t) = 0 \quad \text{otherwise},$$

$$T_i = t \quad \text{if} \quad V_i^t \geqslant \theta, \tag{3.3}$$

where $a_j^t$ takes the value 1 if neuron $j$'s fired at iteration $t$, and 0 otherwise. $B_i^t$ is the realization of a centered Gaussian random variable of variance $\sigma^2$. All the parameter values are the same as for the previous model; we just rescale $t_m$ by dividing it by the sum of the transmission delay value $d$ and the rise time $t_r$ of the EPSP's which were used for the model studied in Sec. II. $n$ is taken to be large ($n=24$), so that $U(n-1)$ is close to zero.

Since we are interested in the dynamics of the activity level $S$, and not in the behavior of an individual neuron, we want to reduce system (3.1) of $N$ equations to a lower-dimensional system easier to study. To this end, we describe the network from a macroscopic point of view. We call $x_k (k \geqslant 1)$ the fraction of neurons having a refractory state $U=U(k)$, where $k$ is an integer. Let $U_i^0$ be the initial refractory state of a given neuron $i$. After $n$ iterations, either neuron $i$ fired at least once and its refractory state is $U(k)$ with $0 \leqslant k < n$, or it did not fire and its refractory state is $U(n)$. Thus, after $n$ iterations, whatever the initial condition was, one can describe the refractory state of the network by the fractions $x_k$ $(1 \leqslant k \leqslant n-1)$ of neurons with $U=U(k)$ and by the fraction $x_n$ of neurons which have not discharged for at least $n$ iterations. The fraction $S$ of spiking neurons is given by

$$S = x_0 = 1 - \sum_{k=1}^{n} x_k . \tag{3.4}$$

We call $X^t=(x_1^t, \ldots, x_n^t)$ the macrostate of a network at iteration $t$. Let $\mu^t$ be the network microstate which consists of the vector $(U_1^t, \ldots, U_N^t)$ of the refractory states of all the $N$ neurons, with $U_i^t = U_m$ if neuron $i$ is firing at $t$. By definition, $X$ is a function of $\mu$. The next macrostate is $X^{t+1} = X(\gamma(\mu^t))$ where $\gamma$ is the operator defined by the connection matrix $[c_{ij}]$ and the distribution probability of the noise $B_i$. Thus to obtain $X^{t+1}$ we need to know both $\mu^t$ and $\gamma$. Moreover, because of the noise $B_i$, $X^{t+1}$ is actually the realization of a random variable. Nevertheless, we can derive, for a given microstate $\mu$, the expected macrostate over the noise probability distribution and over all the networks with parameters $N$ and $K$ as a function of $X$ only. To this end, we define a function $\Phi$ in the following way:

$$\Phi(X(\mu^t)) = \lim_{N\to\infty} E[X(\Gamma(\mu^t))] \tag{3.5}$$

$\Gamma$ is the random operator defined by the noise probability distribution and by the random matrix $[C_{ij}]$, where the $C_{ij}$ are random variables having all the same probability law, i.e. the law that is used when a network is built (see Sec. II). $E$ denotes the expectation with respect to the probability distribution of $\Gamma$. Thus, $\Phi$ gives the next expected macrostate $X^{t+1}$ as a function of $X(\mu^t)$, when $N \to \infty$.

We now derive the components $\phi_k$ $(1<k<n)$ of $\Phi$:

$$E[x_k(\Gamma(\mu^t))] = E\left[\frac{1}{N}\sum_{i=1}^{N} \delta(U_i^{t+1} - U(k))\right] \tag{3.6}$$

$$= \Pr\{U_1^{t+1} = U(k)\} \tag{3.7}$$

$$= \Pr\{(U_1^t = U(k-1)) \cap (U(k) + (J/K) Y_1^{t+1} + B_1^{t+1} < \theta)\}, \tag{3.8}$$

where Pr denotes the probability and $\delta(x)$ equals 1 if $x=0$, and 0 otherwise. $Y$ is the random variable corresponding to the number of elementary inputs received by a neuron. When $N \to \infty$, we have

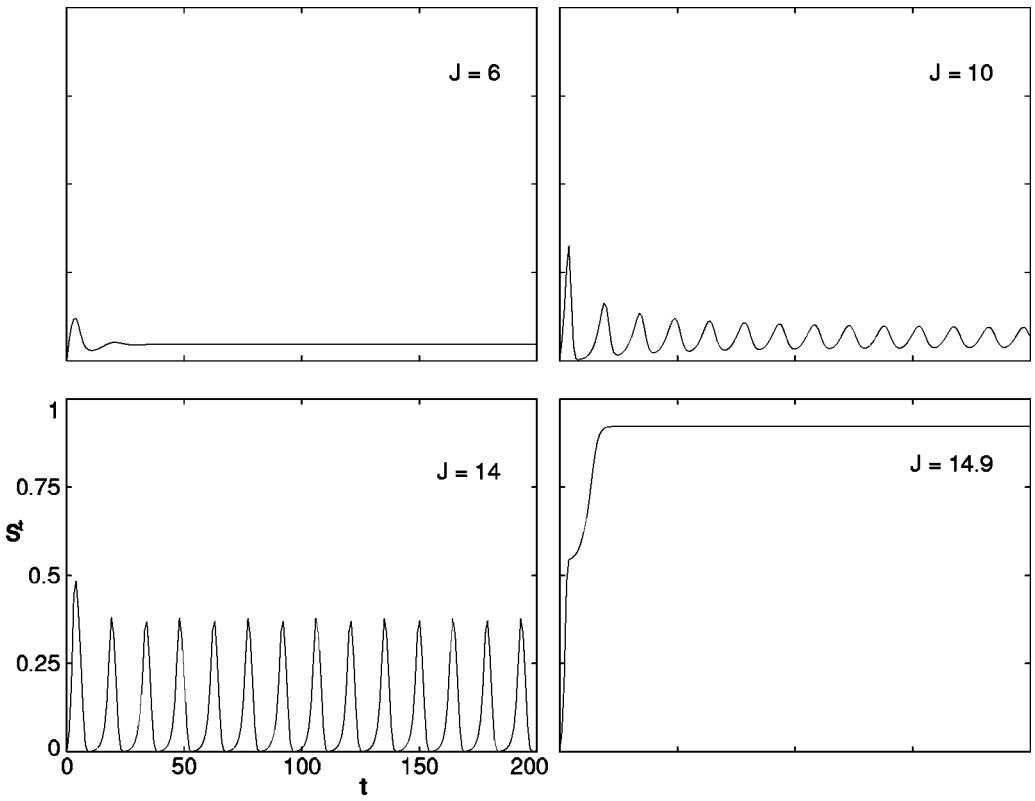


FIG. 7. Dynamics of the activity level $S^t$ (dimensionless) obtained with the map $\Phi$ [Eqs. (3.10)–(3.13)], with $\sigma^2=1.8$ and for different coupling constants $J$. $t$ here is the time in numbers of iteration steps.

$$\phi_k(X(\mu^t))=x_{k-1}^t\sum_{y=0}^{+\infty}\Pr\{Y_1^{t+1}=y\}\times\Pr\{B_1^{t+1}<\theta-U(k)-(J/K)y\} \quad (3.9)$$

and the probability law of $Y$ approaches a Poisson law of parameter $KS$. Thus $\phi_k$ $(1<k<n)$ is given by

$$\phi_k(X(\mu^t))=x_{k-1}^t(1-P_k(S^t)), \quad (3.10)$$

$$P_k(S)=\sum_{y=0}^{+\infty}\frac{(KS)^y}{y!}e^{-KS}\rho(\theta-U(k)-(J/K)y), \quad (3.11)$$

where $\rho$ is the Gaussian repartition function with mean zero and variance $\sigma^2$. In the same way, we derive $\phi_1$ and $\phi_n$:

$$\phi_1(X(\mu^t))=S^t(1-P_1(S^t)), \quad (3.12)$$

$$\phi_n(X(\mu^t))=(x_{n-1}^t+x_n^t)(1-P_n(S^t)). \quad (3.13)$$

$\Phi$ gives the mean macrostate $E[X^{t+1}]$, over all the networks with parameter $K$, as a function of $X(\mu^t)$, when $N\to\infty$. We have now to examine how far from this mean value the macrostates of the individual networks are. Actually, using the properties of the variance, we can show that

$$\lim_{N\to\infty}\mathrm{var}[X(\Gamma(\mu^t))]=0, \quad (3.14)$$

where var denotes the variance with respect to the probability distribution of $\Gamma$. Thus, for a given initial microstate $\mu$ and a large number $N$ of neurons, it is expected that the sequence

$$X^{t+1}=\Phi(X^t) \quad (3.15)$$

provides a good approximation of the dynamics of the macrostate $X$ over at least one iteration. The important point now is that $\mu^t=\gamma^t(\mu^0)$ should also be considered as a random variable. If the microscopic variables $U_i$ $(1\leqslant i\leqslant N)$ are stochastically independent, then one can show that relation (3.15) indeed gives the time course of the macrostate of large networks. Such an independence of the $U_i$ would be obtained, for instance, in a network where the connections are rerandomized at each iteration. Approximating a system, with fixed relations between its units, by a system where these relations are reshuffled during time can lead to a good estimation of the system properties [21]. In the present study, the network connections are fixed during time. Nevertheless, by considering only the asymptotic independence among finite subsets of the microscopic variables, Amari [22] demonstrated that such a map $\Phi$ provides a good approximation of the macrostate dynamics of sparsely connected networks with frozen connections. Moreover, many numerical studies [23], carried out with different models of sparsely connected neural network models, are in agreement with Amari's result. The important result that we want to stress in this paper is that the behavior of the map $\Phi$ that we obtained is in excellent agreement with the networks' simulations presented in Sec. II.

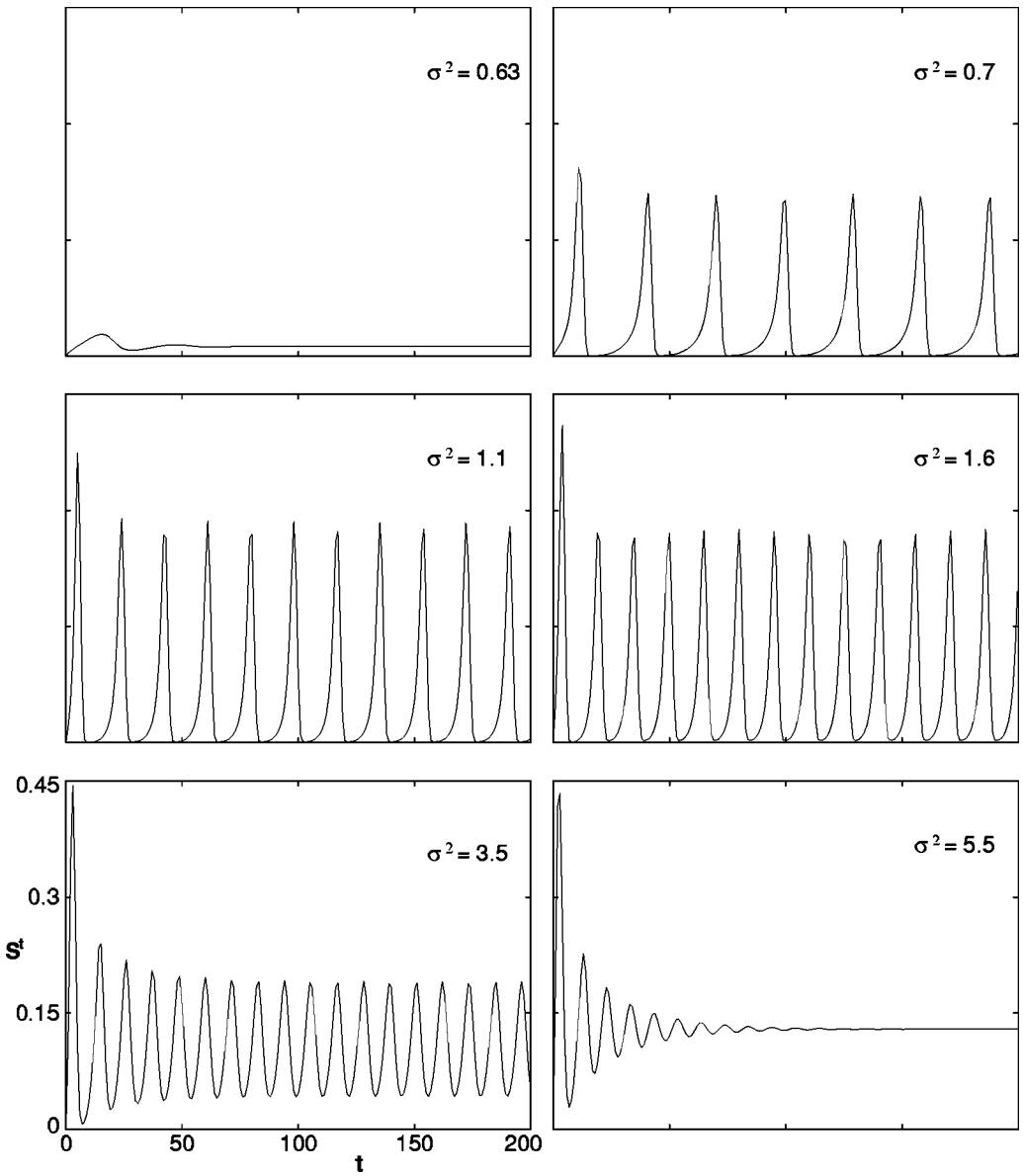


FIG. 8. Dynamics of the activity level $S^t$ (dimensionless) obtained with the map $\Phi$ [Eqs. (3.10)–(3.13)], with $J=12$ and for different noise amplitudes $\sigma^2$. $t$ is the time in numbers of iteration steps.

Indeed, the dynamics of the activity level $S$ computed with the map $\Phi$ have the same dependencies on the coupling strength $J$ and the noise amplitude $\sigma^2$ as those observed in network simulations. Figure 7 shows the effect of the coupling strength $J$, with $\sigma^2=1.8$, on the time course of $S$ obtained with Eqs. (3.10), (3.11), (3.12), and (3.13). With a weak coupling, after a few iterations the activity level remains constant at a low level. As $J$ is raised, oscillations appear and their amplitude increases smoothly with $J$. With strong coupling strengths, the activity rises to a high level at which it remains constant.

Figure 8 shows the effect of the noise amplitude $\sigma^2$ on the activity dynamics when $J=12$. With a very low noise amplitude ($\sigma^2=0.63$) $S$ is maintained constant at a low level. When $\sigma^2$ overtakes a threshold value close to 0.7, oscillations appear brutally with a nonzero amplitude. Then, as $\sigma^2$ is further increased, the frequency of the oscillations monotonously increases. The amplitude increases when $\sigma^2$ is varied from 0.7 to 1.1, and progressively decreases with higher noise levels. Finally, when $\sigma^2$ is greater than 3.95, oscillations disappear. Thus the dynamics of map $\Phi$ have the exact same dependencies on $J$ and $\sigma^2$ as those described for simulated networks in Sec. II.

In the parameter ranges for which oscillations were observed, except for strong values of $J$ or for low values of $\sigma^2$, varying the initial condition $X^0$ did not lead to different behaviors. That is, only oscillations of $S$, and no constant activity levels, were obtained. Therefore, to determine the parameter values allowing oscillations, it is interesting to find the macrostates $X$ such that $S$ will be kept constant over time. Actually, such macrostates are the locally stable fixed points of the map $\Phi$. Indeed, using Eqs. (3.10), (3.11), (3.12), and (3.13), we find that a macrostate $X^*=(x_1^*,\ldots,x_n^*)$, with activity level $S^*=1-x_1^*-\cdots-x_n^*$, is a fixed point of $\Phi$ if it is solution of the nonlinear system:

$$x_k=S\prod_{j=1}^{k}(1-P_j(S)) \quad (1\leqslant k<n),$$

$$x_n = S\prod_{j=1}^{n}(1-P_j(S))/P_n(S). \tag{3.16}$$

System (3.16) can be reduced to a single equation in $S$ by adding all the lines and using the relation $S=1-x_1-\cdots-x_n$. This equation can be solved numerically and, once $S^*$ is obtained, the $x_k^*$ $(1\leqslant k\leqslant n)$ values can be deduced from Eqs. (3.16). Thus, Eqs. (3.16) define a one-to-one correspondence between $X^*$ and $S^*$ which is the activity level kept constant over time when $X^*$ is stable. The local stability of $X^*$ can be studied by linearizing system (3.16) near the fixed point,

$$\Phi(X^*+\Delta)=X^*+J[\Phi(X^*)]\Delta, \tag{3.17}$$

where $J$ is the Jacobian matrix and $\Delta$ a small perturbation. $X^*$ is locally stable if all the eigenvalues of $J[\Phi(X^*)]$ have a modulus less than 1.

For different sets of parameters, the fixed points $X^*$ were computed and their local stability was examined. Figure 9(a) represents the activity level $S^*$ of the fixed points $X^*$ as a function of the coupling $J$, with $\sigma^2=1.8$. Thick continuous lines correspond to the locally stable fixed points, the thin dotted line corresponds to the unstable points, and the thick dashed lines indicate the minimal and maximal values of $S$ when oscillations occur. When $J$ is varied from 0 to 25, the branch of the fixed points presents two successive folds. With a weak coupling, there is only one locally stable fixed point, referred to as **L**, and $S$ is kept constant at a low level. When $J$ is close to 9.6, a Hopf bifurcation occurs [24]. The fixed point loses its stability and oscillations appear with a very small amplitude. As $J$ increases, this amplitude rises. When $J$ is close to 13.85 a locally stable fixed point appears, through a saddle-node bifurcation, with a high activity level. We denote this stable fixed point by **H**. Oscillations are still possible until $J=15.4$. Thus, for $J$ between 13.85 and 15.4, the system is bistable: depending on the initial condition, networks display sustained oscillations or stabilize at a high activity level. At $J=15.4$, oscillations collide with a saddle point and disappear through a saddle-loop bifurcation.

In Fig. 9(b), $J$ is kept constant at 12, and the noise amplitude $\sigma^2$ is varied from 0 to 5. With low noise amplitudes ($\sigma^2<0.7$) there is a locally stable fixed point with a low activity level $S^*$ increasing with $\sigma^2$. When $\sigma^2$ is close to 0.7, a Hopf bifurcation occurs, and oscillations appear with a nonzero amplitude. If $\sigma^2$ is then decreased, oscillations persist until $\sigma^2=0.67$, where they disappear with a nonzero amplitude. Thus, for $\sigma^2$ between 0.67 and 0.7, the system is bistable, as both a stable fixed point and stable oscillations coexist. When $\sigma^2$ increases beyond 0.7 the amplitude of the oscillations rises sharply until $\sigma^2=1.05$, and then progressively decreases. For $\sigma^2=3.95$ the fixed point regains its stability through a second Hopf bifurcation. It should be noted that the characteristics of the oscillations vary with $\sigma^2$ in a way similar to what was obtained with simulated networks (see Fig. 6).

Figures 9(a) and 9(b) show that there is a region of the parameter plane $(J,\sigma^2)$ where the system has no stable fixed points. In this region the system stabilizes into an oscillatory activity. To delimit this region of parameter plane, we computed the values of $J$ and $\sigma^2$ at which the fixed points lose their stability. The result is presented in Fig. 10. Continuous lines partition the parameter plane $(J,\sigma^2)$ into different regions according to the stability of the fixed points. **L** and **H** stand for the region where there exists only one locally stable fixed point with, respectively, low and high activity levels $S^*$. **LH** indicates the bistability region where the two stable fixed points coexist. **O** is the region where oscillation is the only asymptotically stable regime. In region **OH**, depending on the initial condition, the system will either oscillate or maintain a constant high activity level. Thick lines indicate the positions of the two folds presented in Fig. 9(a). The left thick line in Fig. 10 corresponds to the higher fold, where the saddle-node bifurcation takes place, and the right thick line indicates the lower fold. In Fig. 10, the two thin dotted lines represent two new folds that appear at a cusp at $J=13.6$ and $\sigma^2=0.55$, below the lower fold of Fig. 9(a). The lowest of the two new folds takes place at large values of $J$, for low values of $\sigma^2$. Consequently, the branch of the low stable fixed points **L** also extends to larger values than the position

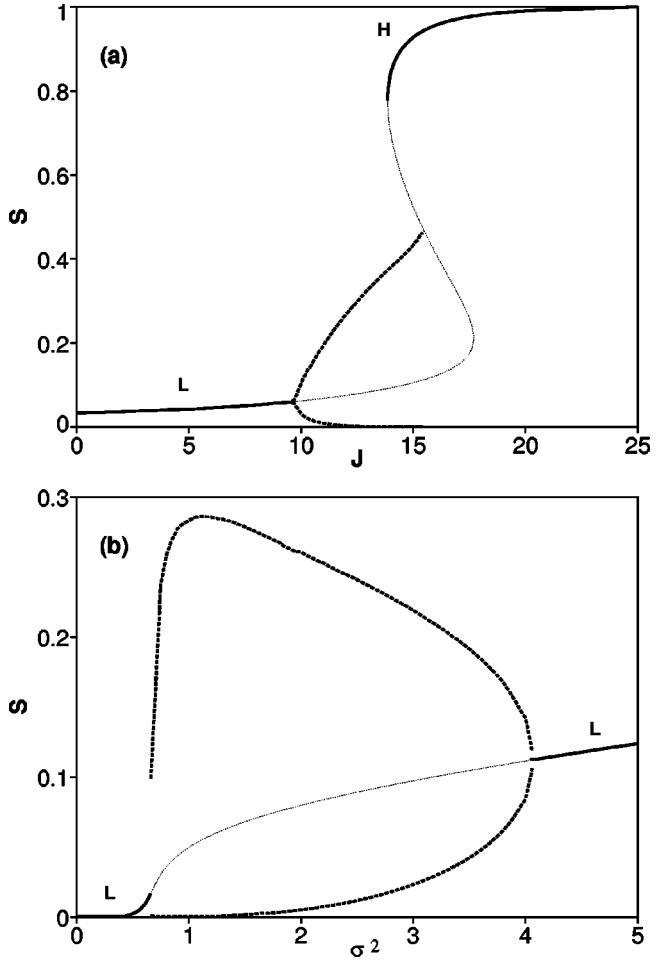


FIG. 9. Activity levels $S^*$ at the fixed points of the map $\Phi$ [Eqs. (3.10)–(3.13)] as a function of the coupling $J$, when $\sigma^2=1.8$ (a), and as a function of the noise amplitude $\sigma^2$, when $J=12$ (b). $S$, $J$, and $\sigma^2$ are dimensionless. Thick solid lines correspond to the locally stable fixed points. **H** stands for locally stable fixed points with a high activity level, and **L** for locally stable fixed points with a low activity level. Thin dotted lines correspond to unstable fixed points, and thick dashed lines indicate the minimal and maximal values of the activity level $S$ when oscillations are present.

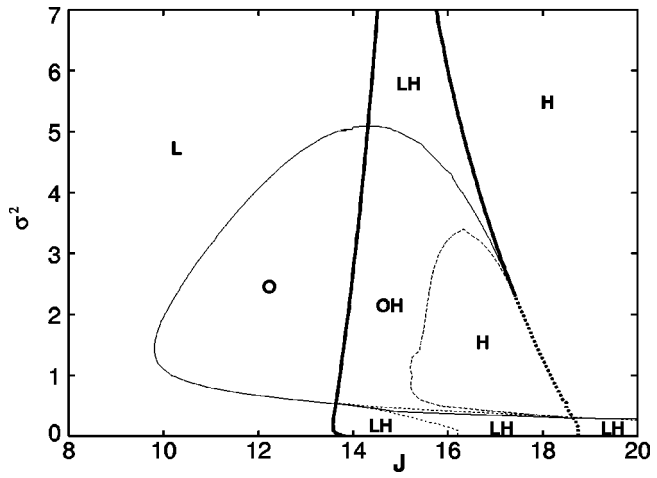


FIG. 10. Stability regions of the different regimes obtained with the map $\Phi$ in the parameter plane $(J,\sigma^2)$ for a sparsely connected network ($K=15$). Both $J$ and $(J,\sigma^2)$ are dimensionless. Solid lines partition the plane according to the local stability of the fixed points. In regions **L** and **H** there is only one locally stable fixed point, with, respectively, a high and low activity level [see Fig. 9(a)]. In region **LH** both stable fixed points coexist. In region **O** only oscillations are asymptotically stable. In **OH** the system either oscillates or settles into a stable fixed point with high activity level. The dashed line is the boundary between **OH** and **H**. The thick left line corresponds the higher fold of Fig. 9(a), and the right thick line to the lower fold of Fig. 9(a).

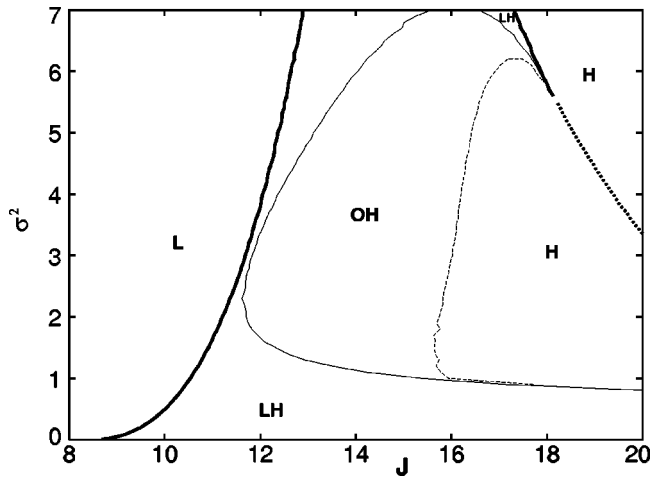


FIG. 11. Stability regions of the different regimes obtained with the map $\Phi$ in the parameter plane $(J,\sigma^2)$ for a fully connected network ($K=N-1$). Same legends as in Fig. 10.

of the lowest fold in Fig. 9(a), when $\sigma^2$ is small.

From Fig. 10, we can draw three conclusions regarding the generation of noise-induced oscillations.

(1) There exists a wide region of the parameter plane $(J,\sigma^2)$ where noise-induced oscillations can occur. Oscillations are not present in the absence of noise (see Fig. 10 when $\sigma^2=0$). This is consistent with what was observed in the network simulations presented in Sec. II. When starting from an oscillating activity (regions **O** or **OH**), if the noise is suppressed, the activity dies out; that is, the system settles into the fixed point **L**, corresponding to $S^*=0$ when $\sigma^2=0$.

(2) Many different scenarii can lead to oscillations. If the system starts from region **L**, with $0.3<\sigma^2<5$, increasing the coupling $J$ will lead to oscillations through the Hopf bifurcation presented in Fig. 9(a). If $\sigma^2$ is less than 3.4, a further increase of $J$ will lead to the disappearance of these oscillations, as in Fig. 9(a), when they collide with a saddle point kicking the system toward the fixed point **H**. If $\sigma^2$ is greater than 3.4, before stabilizing in **H**, the system will first pass through a stable fixed point of type **L**, localized near the lower fold of Fig. 9(a). When starting from region **L**, with $\sigma^2=0$ and $9.81<J<15.2$, increasing only the noise amplitude will make oscillations appear and disappear through the two successive Hopf bifurcations presented in Fig. 9(b).

(3) For such oscillations, induced by varying $\sigma^2$, the situation is quite different when the system does not start from region **L** but rather from the bistable region **LH**. In this case, to obtain oscillations, the initial condition has to be the lower fixed point **L**. When $J$ is greater than 15.2, increasing $\sigma^2$ will lead first to oscillations and then to stabilization into the higher fixed point. Once the network is locked in this higher fixed point, neurons discharge with a high frequency and receive permanently strong inputs. Except when $J$ is close to the left thick line of Fig. 10, varying the noise amplitude only does not allow the system to escape from the fixed point **H**, and the coupling has to be lowered. Switching back and forth from oscillating to nonoscillating regimes is different in regions of monostability than in regions of bistability. In regions **L** and **O**, such switching can be obtained only by varying the system parameters. In region **OH**, changes of the regime can also be obtained by a simple perturbation of the system.

To complete our study of the parameter values allowing oscillations to occur, we have also examined the effect of the network connectivity, i.e., the effect of parameter $K$. This study is presented in Sec. IV, where we consider the case of a fully connected network.

## IV. FULLY CONNECTED NETWORK

We now consider the same network model (3.1) as in Sec. III, with the same parameter values, except for the connectivity parameter $K$ that we set equal to $N-1$. Thus each neuron emits a connection to all the other neurons and receives connections from all the other units. With such a fully connected network, there exists a unique connection matrix $[c_{ij}]$. Consequently, the derivation of the map $\Phi$, which gives the dynamics of the macrostate $X$, is considerably simplified compared to the case of the sparsely connected network. The dynamics of $X$ is described by the same set of equations (3.10), (3.12) and (3.13), but this time with

$$P_k(S)=\rho(\theta-U(k)-JS). \tag{4.1}$$

Simulations of this new map $\Phi$ showed that oscillations were still possible in a fully connected network. We also checked that such oscillations are obtained in simulations of the network model presented in Sec. II, when $K=N-1$. We did the same study of the fixed point stability of the map $\Phi$ as in Sec. III. The results for the fully connected network model are presented in Fig. 11, with the same legends as in Fig. 10. Regions **L** and **H**, where there is only one stable fixed point, are still present, as well as the regions **LH** and **OH** of bistability. The main difference with the sparsely con-

nected network is that there is no longer a region **O** where only oscillations are asymptotically stable. Thus, with this fully connected network, oscillations occur only in regions of bistability. This implies that the generation of noise-induced oscillations depends on the initial condition, and that the oscillation regime is sensitive to perturbations of the activity of the network units. We examined how this result was sensitive to variations of the model parameters. We found that varying the membrane time constant $t_m$, the after-spike hyperpolarization $U_m$ or the firing threshold $\theta$ could lead to the appearance of a region **O** for a fully connected network. The effects of these parameters on the generation of oscillations will be detailed in a further publication. The main result that we want to stress in this paper is that, for a given set of parameters, the region **O**, in which oscillations only are asymptotically stable, is always much wider in a sparsely connected than in a fully connected network. This effect of the connectivity $K$ can be sketched using Fig. 9(a) as follows: for a given value of the noise amplitude $\sigma^2$, when $K$ is increased, the higher fold is moved toward lower coupling constants $J$, whereas the lower fold and the region where the fixed point **L** loses its stability, and where oscillations occur, is moved toward higher values of $J$. So, finally, when the network is fully connected ($K=N-1$), region **O** has become smaller. In other words, the stronger the connectivity is, the more the network is likely to settle into the saturated firing state **H**.

## V. CONCLUSION

We have shown that noise alone can induce synchronization and oscillations in an excitatory network of coupled excitable neuron models. Similar oscillations were first reported by Macgregor and Palasek in simulations of neuron pools [25]. In the present study we have explained how such oscillations are produced. The whole network is an excitable system which responds to an initial noise-induced firing of neurons with a transient amplification of the activity, that we called a burst, followed by a refractory period during which the network is less sensitive to a new stimulation. We have shown that in such an excitable system, the regularity of the oscillations is a nonmonotonic function of the noise amplitude $\sigma^2$. This relies on the differential dependencies on $\sigma^2$ of the interburst interval and the burst duration. Such a mechanism is qualitatively similar to what was proposed by Pikovsky and Kurths for so called ''coherent resonance'' with a single FitzHugh neuron model [12]. Meanwhile, the system we studied here is not a single neuron. Noise is imposed upon a large number of neurons, and a burst is ignited when a fraction of them fires within a short time window. The regularity of the oscillations is therefore not related to the threshold crossing of a single neuron, but to the average noise-induced spiking over a large population. Thus, provided the number of neurons is large, oscillations can be quite regular. To study the dependence of these oscillations on the noise amplitude, we have derived a discrete map which gives the dynamics of large networks. A similar map had been previously studied by Bauer and Pawelzic [26] for the particular case of a fully connected network with transmission delays very short compared to the duration of the neuron refractory period. The map we derived in the present study is more general, and can also account for the dynamics of sparsely connected networks. Moreover, we have not only numerically studied the map dynamics, but have also determined and analyzed its bifurcation structure. This led to the conclusion that noise induced oscillations can occur over wide ranges of the network parameters, and that there exist two different situations for the generation of oscillations. Either oscillating is the only asymptotically stable regime, or it occurs in a parameter region of bistability where the system can also settle into a state of high frequency firing of the neurons. We have shown that sparsely connected networks are more likely than fully connected networks to display oscillations robust to perturbations.

The authors thank D. R. Chialvo, O. Arino, P. Y. Boelle, and H. Fukai for very helpful comments on this work.

[1] J. P. Segundo, J.-F. Vibert, K. Pakdaman, M. Stiber, and O. Diez-Martínez, *Origins: Brain and Self Organization*, edited by K. Pibrom (Lawrence Erlbaum, Hillsdale, NJ, 1994).

[2] H. Spekreijse, Vision Res. **9**, 1461 (1969); A. French, A. V. Holden, and R. B. Stein, Kybernetik **11**, 15 (1970); J.-F. Vibert and J. P. Segundo, Biol. Cybern. **43**, 81 (1979); O. Diez-Martínez, Ph.D. thesis, UCLA, 1981.

[3] O. Macadar, G. Wolfe, D. P. O'Leary, and J. P. Segundo, Exp. Brain Res. **22**, 1 (1975); W. Buno, J. Fuentes, and J. P. Segundo, Biol. Cybern. **31**, 99 (1978).

[4] H. Spekreijse and H. Oosting, Kybernetik **7**, 22 (1970).

[5] J. K. Douglass, L. Wilkens, E. Pantazelou, and F. Moss, Nature (London) **365**, 337 (1993).

[6] J. J. Collins, T. T. Imhoff, and P. Griegg, J. Neurophysiol. **76**, 642 (1996); J. E. Levin and J. P. Miller, Nature (London) **380**, 165 (1996).

[7] A. R. Bulsara, S. Lowen, and C. Reese, Phys. Rev. E **49**, 4989 (1994); A. R. Bulsara, T. C. Elston, C. R. Doering, S. B. Lowen, and K. Lindenberg, *ibid.* **53**, 3958 (1996); A. Longtin, A. R. Bulsara, and F. Moss, Phys. Rev. Lett. **67**, 656 (1991); A. Longtin, J. Stat. Phys. **70**, 309 (1993); X. Pei, K. Bachmann, and F. Moss, Phys. Lett. A **206**, 61 (1995); P. Jung and G. Mayer-Kress, *ibid.* **74**, 2130 (1995); K. Wiesenfeld *et al.*, *ibid.* **72**, 2125 (1994); J. J. Collins *et al.*, Phys. Rev. E **54**, 5575 (1996); D. R. Chialvo, A. Longtin, and J. Müller-Gerking, *ibid.* **55**, 1798 (1997).

[8] A. Longtin, Phys. Rev. E **55**, 868 (1997).

[9] D. Sigeti and W. Horsthemke, J. Stat. Phys. **54**, 1217 (1989).

[10] W. J. Rappel and S. H. Strogatz, Phys. Rev. E **50**, 3249 (1994).

[11] H. Gang, T. Ditzinger, C. Z. Ning, and H. Haken, Phys. Rev. Lett. **71**, 807 (1993).

[12] A. S. Pikovsky and J. Kurths, Phys. Rev. Lett. **78**, 775 (1997).

[13] J. F. Lindner, B. K. Meadows, W. L. Ditto, M. E. Inchiosa, and A. R. Bulsara, Phys. Rev. Lett. **75**, 3 (1995); V. Hakim and W. J. Rappel, Europhys. Lett. **27**, 637 (1994); P. Jung, Phys. Rev. E **50**, 2513 (1994).

[14] Y. Shinomoto and Y. Kuramoto, Prog. Theor. Phys. **75**, 1105 (1986); H. Sakaguchi, Y. Shinomoto, and Y. Kuramoto, *ibid.* **79**, 600 (1988).
[15] C. Kurrer and K. Schulten, Phys. Rev. E **51**, 6213 (1995).
[16] W. J. Rappel and A. Karma, Phys. Rev. Lett. **77**, 3256 (1996).
[17] W. Gerstner and J. L. van Hemmen, Network **3**, 139 (1995).
[18] W. Gerstner, Phys. Rev. E **51**, 738 (1995).
[19] W. Gerstner, J. L. van Hemmen, and J. D. Cowan, Neural Comput. **8**, 1653 (1996).
[20] J. Pham, K. Pakdaman, J. Champagnat, and J.-F. Vibert, Neural Networks **11**, 415 (1998).
[21] B. Derrida and Y. Pomeau, Europhys. Lett. **1**, 45 (1986).
[22] S. Amari, Kybernetik **14**, 201 (1974); S. Amari, K. Yoshida, and K. A. Kanatani, SIAM (Soc. Ind. Appl. Math.) J. Appl. Math. **33**, 95 (1977).
[23] P. A. Anninos, B. Beek, T. J. Csermely, E. M. Harth, and G. Pertile, J. Theor. Biol. **26**, 121 (1970); S. Amari, IEEE Trans. Syst. Sci. Cybern. **2**, 643 (1972); R. Wong and E. Harth, J. Theor. Biol. **40**, 77 (1973); S. Yoshizawa, Kybernetik **16**, 173 (1974); W. Senn, K. Wyler, J. Streit, M. Larkum, H. R. Lüscher, H. Mey, L. Müller, D. Stainhauser, K. Vogt, and T. H. Wannier, Neural Networks **9**, 575 (1996).
[24] G. Iooss, *Bifurcation of Maps and Applications* (Elsevier, New York, 1979).
[25] R. J. MacGregor and R. L. Palasek, Kybernetik **16**, 79 (1974).
[26] H.-U. Bauer and K. Pawelzic, Physica D **69**, 380 (1993); J. Deppisch, H.-U. Bauer, T. Schillen, P. König, K. Pawelzic, and T. Geisel, Network **4**, 243 (1993).